Theor Chem Acc (1999) 102:196–206
DOI 10.1007/s00214980m164

Theoretical
Chemistry Accounts

Regular article

Argon-matrix-isolation Raman spectra and density functional study of 1,3-butadiene conformers*

Cheol Ho Choi[1], **Miklos Kertesz**[1], **Sergey Dobrin**[2], **Josef Michl**[2]

[1] Department of Chemistry, Georgetown University, Washington, DC 20057-1227, USA
[2] Department of Chemistry and Biochemistry, University of Colorado, Boulder, CO 80309-0215, USA

Received: 1 July 1998 / Accepted: 26 October 1998 / Published online: 15 February 1999

Abstract. s-trans, s-cis and gauche conformers of 1,3-butadiene have been studied using density functional theory and the coupled-cluster method using double substitutions (CCD). Matrix isolation Raman and IR data for the minor conformer were obtained and are used in combination with the theoretical results to resolve earlier ambiguities in vibrational assignments. Based on high-quality Hessians, new harmonic stretching force constants are reported for the carbon backbone of *s-trans*-1,3-butadiene. For the minor conformer the best unscaled root mean square error of the calculated frequencies for the s-cis and gauche geometries are 17.5 cm^{-1} and 7.4 cm^{-1}, respectively, primarily due to a better agreement of the gauche results for the vibrations at 983 cm^{-1}, 596 cm^{-1} and 470 cm^{-1} which depend strongly on the torsional angle. Although this points towards the gauche form rather than the s-cis form, the calculated transition dipole moment directions at the CCD/6-311G(d,p) level confirm the earlier conclusion that the minor conformer has C_{2v} symmetry in the matrix. It is concluded that either the better agreement between the frequencies calculated for the gauche form and the observed values is coincidental, or that the molecule is indeed nonplanar in the matrix and tunnels very rapidly between the two mirror-image forms (or its lowest vibrational level lies above the barrier).

Key words: 1,3-butadiene – Conformers – Raman spectroscopy – Matrix isolation – Density functional theory

1 Introduction

1,3-Butadiene, one of the simplest π-conjugated hydrocarbons, is an important model system for theoretical and experimental studies. The conformation of the minor conformer has attracted much attention. Michl and coworkers [1–3] have found evidence from polarized IR spectra for the s-cis conformation of the minor conformer, supporting an earlier UV absorption study [4], while other evidence [5, 6] favored a gauche conformation with a sizable deviation from planarity with respect to the torsional (τ) angle around the C—C single bond. Still other evidence [7] is more ambiguous concerning the conformation of the minor component, as discussed below. Nevertheless, the evidence based on experimental transition dipole moment directions [1–3] is particularly noteworthy, because it is sensitive to the conformation and it can be tested theoretically for the major component (s-trans).

Theoretically, Wiberg and Rosenberg [8] have shown that the gauche conformer is energetically preferred by 0.98 kcal/mol with MP3/6-311+G*//MP2/6-31G*. Their calculated vibrational spectra for the minor rotamer are in better agreement with the gauche conformation and their assignment of $\lambda_{\max}$ of the UV/VIS data, though somewhat ambiguous, is in agreement with a dihedral angle (τ) near 25–35°. Meanwhile, by using an experimentally derived force field, Furukawa et al. [7] have pointed out that most of the infrared bands due to the second stable conformer can be reasonably assigned by assuming either the gauche or the cis conformation. Therefore, any conclusion merely based on statistics of the frequency fit should be evaluated carefully.

Concerning energetics, Guo and Karplus [9] have also predicted the second stable conformer of butadiene to be a gauche conformation with a dihedral angle between 35° and 40° and a barrier of 0.5–1.0 kcal/mol to the s-cis transition state, on the basis of Hartree–Fock (HF) and Møller–Plesset second-order (MP2) levels of calculation. A larger value of 2.8 kcal/mol was obtained by a G2 calculation of Murcko et al. [10]. Feller and Davidson [11], however, have commented that any predictions made by using such small energy differences should be viewed with a certain amount of skepticism. Kofranek et al. [12] have shown that the s-cis structure is stabilized by the matrix cage and the relative cis/gauche stability is inverted, based on the molecular dynamics simulation of

---

*Contribution to the Kenichi Fukui Memorial Issue

Correspondence to: M. Kertesz, J. Michl the influence of an Ar matrix, showing the significance of matrix effects. Unfortunately, the effect of the matrix on the spectrum has not been studied yet. The remaining theoretical work has been done on isolated molecules, including the calculations of this work.

Apart from the planarity issue of the minor conformer, there have also been some inconsistencies in the earlier normal mode assignments. In addition to the known [7, 13–15] IR peak at 537 cm^{-1} assigned to an a_u mode of *trans*-1,3-butadiene, Fisher and Michl [1] observed a very weak peak at 530 cm^{-1} and assigned it as a b_2 mode of *s-cis*-1,3-butadiene. Furukawa et al. [7] proposed that the very weak peaks at 983 cm^{-1} and 727 cm^{-1} are better accounted for by assuming the gauche form, while Fisher and Michl [1] attributed the peak at 727 cm^{-1} to an a_2 mode made weakly allowed by matrix-induced mixing of fundamental modes.

Another important issue is connected to the accurate determination of the force field in *trans*-1,3-butadiene. A great number of studies have been devoted to the predictions of this force field in pursuit of reliable oligoene and polyene force fields. Since the force constants predicted by ab initio HF calculations are not quantitatively acceptable, scaling procedures [16] have been widely utilized. These scaling procedures correct for the error in the HF force constants caused by neglect of electron correlation and anharmonicity [8]. The scaling factors are usually found to be smaller than 1. Szalay et al. [17], however, have found that the C—C/C=C and C=C/C=C off-diagonal force constants obtained by the scaled HF method are significantly smaller in magnitude than those in the corresponding scaled coupled-pair functional (CPF) method case when the standard scaling method is used. Clearly, the fine details of electron correlation effects are rather complex. Guo and Karplus [9] have also shown that while other force constants are overestimated by the HF calculations, the C—C/C=C and C=C/C=C off-diagonal force constants are likely to be underestimated based on the comparison of HF and MP2 calculations. Kofranek et al. [18] applied the averaged CPF (ACPF) method and found that the magnitude of the C=C/C=C coupling constant can be as large as −0.184 mdyne/Å (unscaled). All these studies have suggested that the off-diagonal force constants obtained by HF have to be scaled separately with scaling factors larger than unity [19].

Contradicting evidence was found in the extensive study of an experimental force field as obtained with 131 observed infrared and Raman frequencies of six isotopomers of *s-trans*-1,3-butadiene by Tang and Bally [20]. They found that rather small CC/CC coupling constants such as −0.047 and −0.100 mdyne/Å are consistent with the experimental frequencies. Similarly, Vijay and Sathyanarayana [21] have used their RECOVES procedure for the force constants of butadiene and suggested a small (−0.097 mdyne/Å) C=C/C=C coupling force constant. Recently Lee et al. [22] have also calculated the force fields of *s-trans*-1,3-butadiene with MP2 and MP4 (fourth order) using various basis sets and suggested a relatively small C=C/C=C off-diagonal force constant (−0.11 mdyne/Å). It should be noted that even though they have successfully introduced an "exponential scaling procedure" for vibrational frequencies, their technique does not yield a new set of scaled force constants.

Density functional theory (DFT) [23] in the current practice [24–26] includes substantial electron correlation effects and offers accurate a priori prediction of vibrational properties. In this study, DFT methods in combination with various basis sets were applied to the a priori predictions of vibrational properties of 1,3-butadiene. At the same time, matrix isolation Raman experiments were performed on the minor conformer of 1,3-butadiene. With the help of the excellent predictions of vibrational properties of *s-trans*-1,3-butadiene, we first suggest realistic carbon backbone harmonic force constants including the C—C/C=C and C=C/C=C off-diagonal force constants of *s-trans*-1,3-butadiene. After that, an attempt to resolve some of the inconsistencies in the normal mode assignments for the minor conformer on the basis of the new Raman data in combination with the calculations is made. Finally, we comment on the planarity of the minor conformer.

2 Experimental and computational details

1,3-Butadiene (Matheson) and argon (Scott Specialty Gases) showed no impurities in the IR and Raman spectra. Argon/butadiene mixtures were deposited at a flow rate of about 0.05 mol/h onto a cold (20 K) sample holder mounted on an Air Products Displex closed-cycle helium cryostat. For IR measurements (Nicolet 800 FT-IR spectrometer, 1 cm^{-1} resolution) the substrate was a CsI window and the matrix ratio was varied between 1/200 and 1/5000, with identical results (deposition times, 20–30 min). For the Raman measurements the substrate was a nickel-plated copper plate, the matrix ratio was 1/50 as in ref. [7], and the deposition times were at least 1 h. The Raman spectra were recorded with a SPEX 1404 0.85 m double monochromator whose exit slit was replaced with a liquid nitrogen cooled change-coupled device detector, under excitation with the filtered 514.5 nm line of a Coherent Innova 300 argon ion laser, using *f*2 collection optics and a holographic notch filter. The laser power was varied from 10 mW to 1 W. Positions of strong peaks were independent of laser intensity and matrix deposition time. Weak peaks were observed only after long deposition (up to 5 h) and at high laser intensities (1 W).

Samples enriched in the minor conformer were produced by passing the deposition gas mixture through a 10 cm-long quartz tube of 0.9 cm internal diameter, filled with quartz fibers and maintained at 1100 K. Photodestruction of the minor conformer was achieved by irradiation of the matrices with 248 nm light from a Lambda Physics EMG-50 excimer laser (10 mJ per pulse, repetition rate: 2 Hz, irradiation times: 10–60 min). Matrix annealing involved careful heating to 40–45 K. All spectra were reproduced at least 3 times. The results for *s-trans*-1,3-butadiene were essentially identical with those of Furukawa et al. [7], except that one additional peak was observed at 151 cm^{-1} (Table 1).

All density functional calculations were performed by the Gaussian 94 [25] program with the linear combination of the Gaussian-type orbital-DFT method. The Vosko, Wilk and Nusair (VWN) [27] correlation functional was used for the local spin density approximation. Lee, Yang, and Parr's (LYP) [28] correlation functional, and Becke's 1988 (B) [29] and his three parameter hybrid (B3) [30] exchange functionals were used for the nonlocal density approximation. These density functional methods were performed with double-zeta and triple-zeta quality of basis sets augmented with polarization and diffuse functions.

The coupled-cluster method using double substitutions (CCD) in combination with a 6-311G(d,p) basis set was used to predict the transition dipole moment directions.

Table 1. Calculated and experimental frequencies of *s-trans*-1,3-butadiene (in cm^{-1}). The numbers in parentheses are root mean square (*rms*) values without CH stretching modes

	B3LYP			BVWN		MP2		MP4		CPF (scaled)[c]	
	6-31G(d,p)	6-311G(d,p)	6-311G(2d,p)	6-31G(d,p)	6-311G(d,p)	6-311G(d)[a]	6-311G(2d,p)[b]	6-31G[b]	6-31G(d)[b]	DZP	TZP
a_g	3244	3219	3218	3198	3177	3284	3273	3205	3252	3098	3099
	3158	3135	3135	3115	3097	3178	3177	3117	3165	3026	3027
	3144	3122	3122	3095	3080	3189	3166	3093	3149	3014	3008
	1725	1706	1705	1663	1645	1719	1706	1687	1721	1650	1656
	1486	1474	1481	1473	1464	1495	1494	1514	1504	1447	1447
	1323	1314	1319	1305	1299	1325	1318	1333	1328	1287	1291
	1234	1227	1230	1213	1207	1248	1234	1245	1250	1214	1214
	904	899	902	886	882	914	908	897	912	877	880
	517	519	521	509	512	521	517	518	515	522	515
b_u	3245	3220	3219	3199	3177	3284	3273	3205	3252	3099	3099
	3158	3136	3135	3114	3095	3192	3180	3116	3165	3026	3033
	3153	3132	3132	3106	3091	3182	3170	3100	3156	3022	3010
	1672	1653	1656	1624	1607	1651	1646	1633	1657	1588	1591
	1426	1415	1420	1408	1400	1429	1428	1443	1435	1380	1380
	1321	1320	1326	1313	1311	1335	1319	1350	1338	1297	1303
	1006	1004	1010	998	997	1016	1007	1030	1017	994	993
	299	301	303	299	302	298	296	297	295	303	299
b_g	1002	1000	998	978	976	974	988	966	981		
	934	937	937	900	907	908	916	906	901		
	782	781	783	762	762	754	778	742	759		
a_u	1062	1057	1054	1043	1038	1022	1050	1015	1035		
	930	936	936	896	905	905	916	907	900		
	540	539	538	526	525	535	538	517	529		
	178	175	175	179	174	163	169	147	160		
Rms	75.1	62.3	62.9	47.4	37.6	89.4	82.8	56.1	80.5	13.5	10.5

Table 1 (Contd.)

	BLYP							Exp.[d]	Exp.[e]	Exp.[f]
	6-31G(d,p)	6-311G(d,p)	6-311 + G(d,p)	6-311G(2d,p)	6-311G(2d,2p)	6-311G(3d,p)	6-311G(3df,p)			
a_g	3162	3140	3140	3139	3144	3138	3140	3105	3101[g]	
	3078	3057	3057	3058	3063	3056	3050	3025	3014[g]	
	3057	3039	3040	3038	3044	3037	3039	3014	3014[g]	
	1656	1636	1630	1635	1636	1633	1638	1644	1643[g]	1644
	1450	1438	1437	1444	1447	1440	1441	1441	1442[g]	1441
	1287	1279	1278	1284	1286	1280	1284	1279	1291	1280
	1203	1195	1194	1198	1199	1195	1198	1206	1205[g]	1205
	882	877	875	878	878	876	878	887	890[g]	889
	505	508	507	509	509	508	510	513	513[g]	513
b_u	3163	3140	3141	3140	3144	3138	3141	3103	3102[g]	
	3076	3056	3056	3057	3062	3055	3059	3062	3056[g]	
	3067	3051	3052	3050	3055	3048	3051	2986	2985[g]	
	1614	1595	1588	1596	1597	1593	1599	1597	1596	
	1389	1379	1377	1383	1385	1379	1382	1381	1380	
	1290	1287	1287	1293	1295	1288	1291	1294	1282	1299
	981	980	980	986	987	981	983	988	987	
	293	296	296	298	298	297	298	301	303	
b_g	966	961	958	960	966	963	969	974	967[g]	973
	889	893	896	894	897	893	900	908	911[g]	
	757	756	753	757	759	757	760	754	753[g]	756
a_u	1032	1024	1018	1022	1028	1025	1028	1022	1013	
	885	891	895	892	895	890	897	905	908	907
	525	523	521	522	524	523	526	535	525[g]	534
	180	175	173	176	176	176	176	163[h]	163	151
Rms	28.7	19.5	19.9	19.1	21.0	18.7(8.9)	19.1			

[a] Taken from Refs. [9,10]
[b] Taken from Ref. [22]
[c] Taken from Ref. [17]
[d] Taken from Ref. [7] (All rms values are based on these data)
[e] Taken from Ref. [15]
[f] This work, Raman experiment in Ar matrix (18 K)
[g] Taken from Ref. [14]
[h] Taken from Ref. [3]

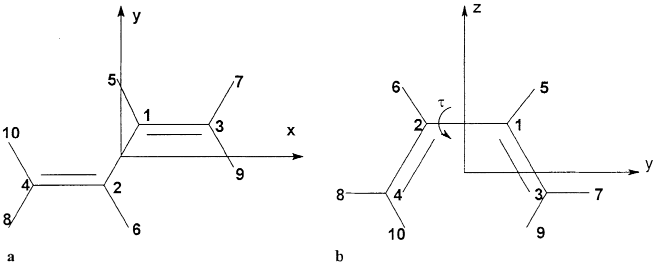

Fig. 1. Molecular orientation and atom numbering of **a** *s-trans*-1,3,-butadiene and **b** *s-cis*-($\tau = 0$) and *gauche*-($\tau \neq 0$) 1,3,-butadiene

All vibrational frequency calculations were made using the fully optimized geometry for each computational method, except in the τ-dependent calculations, where all parameters other than τ were optimized. The definitions of the internal coordinates of *s-trans*-1,3-butadiene suggested by Furukawa et al. [7] were used. The force constants of 1,3-butadiene were transformed into internal coordinates based on these definitions. The atomic polar tensors (APT) [31] determine the infrared intensities in the electric harmonic approximation and are defined as the dipole moment derivatives in Cartesian coordinates for the αth atom

$$\mathbf{P}_X^{\alpha} = \begin{pmatrix} \frac{\partial p_x}{\partial X_\alpha} & \frac{\partial p_x}{\partial Y_\alpha} & \frac{\partial p_x}{\partial Z_\alpha} \\ \frac{\partial p_y}{\partial X_\alpha} & \frac{\partial p_y}{\partial Y_\alpha} & \frac{\partial p_y}{\partial Z_\alpha} \\ \frac{\partial p_z}{\partial X_\alpha} & \frac{\partial p_z}{\partial Y_\alpha} & \frac{\partial p_z}{\partial Z_\alpha} \end{pmatrix} \tag{1}$$

where p_i is the ith component of the total molecular dipole moment.

Molecular orientations are defined in Fig. 1. All the dipole moment derivatives were obtained via the analytical first derivative with respect to the atomic coordinates [25].

The "fine grid" defined as having 75 radial shells and 302 angular points per shell is now a default in the Gaussian 94 package [25]. In all reported calculations, we have used the "fine grid" default option.

3 Results and discussion

3.1 The major conformer of butadiene: frequencies

We first present the computational results of the trans conformer of 1,3-butadiene. Theoretical harmonic frequencies of *s-trans*-1,3-butadiene obtained from several combinations of density functionals and basis sets are presented in Table 1 together with results of earlier theoretical studies and compared with the observed frequencies [7, 13–15]. The unscaled CCD frequencies are too poor to be reported. Most of the DFT results agree better with experimental values than do those of MP2 and MP4. Irrespective of the basis set used, among density functionals, the BLYP exchange-correlation functional gives the best agreement with the experimental frequencies. The BLYP/6-311G(3d,p) method gives remarkably accurate results with an unscaled root mean square (rms) of 18.7 cm^{-1} (excluding the C—H stretching modes, the rms is 8.9 cm^{-1}). The agreement would be even better if experimental harmonic frequencies were used [9, 10]. Further inclusion of diffuse and polarization functions beyond the triple-zeta quality of basis set does not much improve the fit.

3.2 The major conformer of butadiene: force constants

Based on these accurate results, an attempt to suggest more reliable carbon backbone stretching force constants of *s-trans*-1,3-butadiene is made, and these force constants are given in Table 2. The numbers in parentheses are scaled values using the traditional Pulay scaling scheme [16] except for the HF/MIDI-4 [19] case, where separate off-diagonal scaling factors were also used.

Let us discuss the four columns in Table 2 in turn. Our C—C force constants calculated with the BLYP functional reproduced quite well the scaled values of the HF/MIDI-4 [19] method, which might be the best scaled values available. However, compared with the experimental C—C force constants of Furukawa et al. [7], our calculated values are small but close to the experimental value of Tang and Bally [20]. As Wiberg and Rosenbreg [8] have noted, the force constants of Furukawa et al. [7] resulted in large measure from the necessity of setting many of the off-diagonal terms equal to zero. Furthermore, during the optimization of the empirical force constants, Furukawa et al. [7] used fixed values for the C—C/C=C and the C=C/C=C coupling constants taken from ab initio results (Table 2). The unscaled post-HF C—C force constants obtained by several methods are very similar to the experimental force constant and strongly deviate from the best scaled HF force constants. Since these unscaled post-HF force constants yield very large rms values, the empirical C—C force constant is not reliable. Rather, our a priori C—C stretching force constants calculated with DFT seem to be more realistic.

The C=C stretching force constants calculated with various DFTs lie between the experimental and other scaled ab intio force constants. All theoretical and experimental values of the C=C force constant fall between 8.41 and 8.89 mdyne/Å except the value of the scaled HF/6-31G(d) calculation [8] which seems to be too low.

The C—C/C=C coupling constants are rather insensitive to the electron correlation effects within HF and MP2 or MP4 methods; however, they are sensitive to the presence of polarization functions. Inclusion of polarization functions increases the C—C/C=C coupling constant by 10–20% at HF and MP levels of theory. ACPF [18], a method comparable to the configuration interaction method with single and double excitations, has yielded an even larger C—C/C=C coupling constant. An increase in the C—C/C=C coupling has also been observed when doubly excited configurations were included in a PPP study [32]. Our DFT calculation gives larger values than the MP calculations but smaller values than ACPF. The fact that the scaling procedure reduces the magnitude of the C—C/C=C coupling force constant by about 10% if no separate off-diagonal scaling factors are introduced, shows that the scaling procedure somehow yields uneven force constants. Hence, the DFT values are likely to be accurate.

The absolute values of C=C/C=C coupling constants are slightly larger with the MP method compared to the HF values. Furthermore, the C=C/C=C coupling

Table 2. Carbon backbone stretching force constants of *s-trans*-1,3-butadiene (in mdyne/Å). The numbers in parantheses are scaled values

	C—C	C=C	C—C/C=C	C=C/C=C
Exp.[a]	5.428	8.886	0.4[l]	−0.1[l]
HF/6-31G[b]	5.973 (5.087)	11.258 (8.521)	0.372 (0.299)	−0.092 (−0.069)
HF/6-31G(d)[c]	5.85 (4.93)	11.17 (8.01)	0.44 (0.34)	
MP2/6-31G[b]	5.363	9.158	0.354	−0.105
MP4/6-31G[d]	5.154	8.900	0.361	−0.114
MP4/6-31G(d)[d]	5.491	9.263	0.409	−0.116
MP2/6-311+G(d)[d]	5.544	9.182	0.421	−0.107
MP2/6-311++G(d,p)[d]	5.541	9.171	0.418	−0.107
MP2/6-311G(2d,p)[d]	5.434	9.164	0.443	−0.111
CPF/DZP[e]	5.608 (4.974)	9.549 (8.415)	0.461 (0.408)	−0.136 (−0.120)
CPF/TZP[e]	5.360 (4.995)	9.183 (8.497)	0.445 (0.413)	−0.131 (−0.121)
ACPF[f]	5.576	9.329	0.527	−0.184
HF/MIDI-4[g]	(5.159)	(8.888)	(0.451)	(−0.172)
PPP-DCI[h]	(5.513)	(8.530)	(0.701)	(−0.133)
Exp.[i]	5.203	8.873	0.445	−0.047
MP2/6-31G(d)[i]		(8.753)	(0.374)	(−0.100)
MP2/6-31G(d)[j]	(5.112)	(8.627)	(0.372)	(−0.099)
RECOVES-HF/DZP[k]	4.963	8.758	0.442	−0.097
BLYP 6-31G(d,p)[m]	5.109	8.800	0.495	−0.167
6-311G(d,p)[m]	5.019	8.641	0.507	−0.164
6-311+G(d,p)[m]	4.997	8.555	0.509	−0.157
6-311G(2d,p)[m]	4.962	8.605	0.522	−0.161
6-311G(2d,2p)[m]	4.957	8.607	0.521	−0.161
6-311G(3d,p)[m]	4.987	8.584	0.515	−0.162
6-311G(3df,p)[m]	5.010	8.680	0.518	−0.162

[a] Taken from Ref. [7]
[b] Taken from Ref. [33]
[c] Taken from Ref. [8]
[d] Taken from Ref. [22]
[e] Taken from Ref. [17]
[f] Taken from Ref. [18]
[g] Taken from Ref. [19]
[h] Taken from Ref. [32]
[i] Taken from Ref. [20]
[j] Approximate ab initio values taken from Ref. [35]
[k] Taken from Ref. [34]
[l] Taken from Ref. [35]
[m] This work

constants are insensitive to the basis sets and to the order of the MP method. The absolute values of the DFT C=C/C=C coupling force constants are close to the best scaled values (HF/MIDI-4) but larger than those of the other calculations. This observation supports the quality of our BLYP force constants. Considering the small rms of the best BLYP predicted vibrational frequencies, anharmonicity, the electron correlation effects and uncertainties in optimizing scaling factors in multidimensional space, our a priori predicted carbon backbone stretching force constants seem to be realistic.

The elements of the theoretical and experimental APT of *s-trans*-1,3-butadiene are presented in Table 3. There are sign disagreements in the predictions of the xy component of C_1 and the xx component of H_7 compared with experiment. Except for these small components, the DFT values compare quite satisfactorily with experiment. While the predicted APTs are rather insensitive to the presence of polarization functions, inclusion of diffuse functions increases the zz components of all atoms and affects the infrared intensities of out-of-plane modes (Table 4).

Theoretical and experimental infrared intensities are presented in Table 4. It can be seen that inclusion of diffuse function leads to an overestimation of all out-of-plane mode intensities. The predicted intensity of the 2986 cm^{-1} mode ($C_1{-}H_5$ and $C_2{-}H_6$ stretching) is overestimated by a factor of 2–3 for all basis sets. These results are mainly attributed to the overestimation of the in-plane APT components of the H_5 and H_6 atoms (Table 3). Except for these discrepancies, the predicted intensities are in quite good overall agreement with experiment.

The calculated and experimental transition dipole moment directions of *s-trans*-1,3-butadiene are presented in Table 5. The directions calculated with DFT are not in good agreement with experiment. However, the CCD results are in good agreement with the experimentally observed transition dipole directions as were previous HF and MP2 calculations with similar basis sets [2]. This lends strong support to the transition-moment based argument in favor of the s-cis conformation of the minor component in matrix isolation.

3.3 The minor conformer of 1,3-butadiene

Theoretical and experimental [1, 7, 15] vibrational frequencies of *s-cis*- and *gauche*-1,3-butadiene are presented in Table 6 together with the results of earlier calculations.

The Raman spectrum of the minor conformer (Figs. 2–4, Table 6) was obtained in the 100–3600 cm^{-1} region by comparison of Ar matrix-isolation spectra obtained after (1) deposition of room-temperature gas, (2) deposition of hot gas, and either (3) 248-nm irradiation, or (4) annealing of the matrix resulting from the hot deposition, with the same results. The minor conformer was detectable only in matrices obtained by deposition of hot gas. The comparison of hot and cold deposited matrices (Fig. 2) revealed 11 peaks between 100 and 2000 cm^{-1}. After irradiation or annealing, the strongest peaks of the minor conformer at 584, 1428 and 1613 cm^{-1} clearly disappeared. The weaker peaks presumably disappeared as well, but the noise level in the spectra of the transformed matrices was too high to detect this disappearance with certainty. The effects of irradiation and annealing on the largest peak in the spectrum of the minor conformer (1613 cm^{-1}) are compared in Figs. 3 and 4. No peaks of the minor conformer could be distinguished in the C—H stretching region (2900–3400 cm^{-1}).

Table 3. Calculated and experimental atomic polar tensors of *s-trans*-1,3-butadiene (in *e*)

		BLYP							"Exp" [a]
		6-31G(d,p)	6-311G(d,p)	6-311+G(d,p)	6-311G(2d,p)	6-311G(2d,2p)	6-311G(3d,p)	6-311G(3df,p)	
C_1	*xx*	0.110	0.127	0.169	0.128	0.129	0.132	0.133	0.113
	xy	−0.016	−0.008	0.017	−0.002	−0.002	0.004	0.004	0.003
	yx	0.075	0.067	0.072	0.069	0.067	0.062	0.062	0.094
	yy	0.141	0.133	0.129	0.124	0.127	0.117	0.117	0.109
	zz	−0.064	−0.111	−0.133	−0.100	−0.100	−0.111	−0.111	−0.115
C_3	*xx*	−0.093	−0.125	−0.175	−0.122	−0.121	−0.122	−0.121	−0.122
	xy	−0.059	−0.068	−0.089	−0.067	−0.067	−0.068	−0.068	−0.052
	yx	−0.112	−0.112	−0.113	−0.113	−0.113	−0.107	−0.107	−0.101
	yy	0.105	0.110	0.097	0.107	0.111	0.111	0.113	0.067
	zz	−0.286	−0.296	−0.304	−0.280	−0.273	−0.261	−0.260	−0.256
H_5	*xx*	−0.019	−0.015	−0.014	−0.016	−0.015	−0.016	−0.016	−0.008
	xy	0.087	0.090	0.087	0.084	0.085	0.081	0.081	0.069
	yx	0.033	0.038	0.035	0.037	0.038	0.039	0.039	0.013
	yy	−0.098	−0.093	−0.089	−0.088	−0.091	−0.086	−0.086	−0.063
	zz	0.100	0.130	0.138	0.120	0.120	0.121	0.120	0.120
H_7	*xx*	−0.007	0.001	0.005	−0.000	−0.001	−0.002	−0.003	0.004
	xy	−0.049	−0.049	−0.046	−0.043	−0.044	−0.041	−0.041	−0.050
	yx	−0.074	−0.084	−0.082	−0.082	−0.084	−0.080	−0.080	−0.088
	yy	−0.063	−0.063	−0.055	−0.060	−0.062	−0.060	−0.061	−0.050
	zz	0.123	0.136	0.148	0.126	0.122	0.121	0.121	0.145
H_9	*xx*	0.009	0.013	0.016	0.010	0.009	0.008	0.008	0.015
	xy	0.037	0.036	0.032	0.028	0.029	0.024	0.024	0.023
	yx	0.078	0.091	0.088	0.089	0.091	0.086	0.086	0.080
	yy	−0.085	−0.087	−0.082	−0.083	−0.085	−0.082	−0.083	−0.067
	zz	0.127	0.142	0.151	0.134	0.132	0.130	0.130	0.109

[a] Taken from Ref. [8]

Table 4. Calculated and experimental infrared intensities of *s-trans*-1,3-butadiene (in km/mol)

		BLYP							Exp[a]
		6-31G(d,p)	6-311G(d,p)	6-311+G(d,p)	6-311G(2d,p)	6-311G(2d,2p)	6-311G(3d,p)	6-311G(3df,p)	
b_u	3103	35.7	36.5	30.5	31.5	33.3	30.1	30.7	28.5
	3062	11.0	13.1	10.7	15.9	16.0	13.1	13.7	12.8
	2986	33.4	32.4	30.0	26.3	28.6	27.2	27.0	10.9
	1597	11.4	16.6	23.7	16.0	16.2	15.4	15.2	17.33
	1381	1.9	3.3	2.8	2.5	2.5	2.3	2.4	2.96
	1294	2.0	2.4	2.5	2.6	2.4	2.5	2.5	1.94
	988	1.8	2.0	2.0	1.6	1.6	1.4	1.3	1.7
	301	2.3	2.4	2.4	2.5	2.5	2.3	2.3	
a_u	1013	22.5	34.5	38.6	30.1	29.4	30.6	29.8	32.4
	908	64.9	77.7	88.6	68.2	65.4	62.4	62.5	63.01
	525	6.3	10.8	13.2	9.1	8.8	9.2	9.0	16.18
	163	0.2	0.4	0.8	0.3	0.3	0.4	0.5	

[a] Taken from Ref. [8]

We believe that the earlier disagreements concerning mode assignments have now been settled and do not need to be revisited. The assignments and references are summarized in Table 6. The following comments seem pertinent

1. There are two vibrations whose frequencies differ in the Raman and IR spectra more than we can attribute to experimental error. They are the ν_{23} mode located at 1087 cm^{-1} in the IR spectrum (b_2 symmetry from polarization measurement) and at 1089 and 1102 cm^{-1} in the Raman spectrum, and the ν_{24} mode, observed at 596 cm^{-1} in the IR spectrum (a_1 or b_1 from polarization work) and at 584 cm^{-1} in the Raman spectrum. In each case, only a single calculated fundamental mode can be assigned to both frequencies. In view of the excellent general agreement of the calculations with observations, we consider it highly unlikely that the calculations are sufficiently wrong for two distinct fundamentals to be involved in either case. It seems more likely that we are observing separate components of Fermi doublets or matrix site effects, and further work will be necessary before the discrepancy can be resolved.

2. A 983 cm^{-1} vibration observed as a very weak Raman band, and also observed weakly at 984 cm^{-1} in the IR spectrum (a_1 or b_1 symmetry from polarization work), is located just below a 996 cm^{-1} vibration that is intense in the IR spectrum (and also of a_1 or b_1 symmetry). This order is reproduced quite nicely by our

Table 5. Calculated and experimental IR transition dipole moment directions of in-plane (b_u) vibrations of *s-trans*-1,3-butadiene[a]

I	ν^b (cm)	$\lvert\text{Exp}\rvert^b$	BVWN 6-31G**	BLYP 6-311G**	BLYP 6-311G(3d,p)	CCD 6-311G**
1	3082	68	−71	−72	−72	−69
2	3043	74	−84	−83	−82	−71
3	2970	54	19	28	29	56
4	1590	21	10	11	11	12
5	1374	38	75	46	55	42
6	1290	59	70	86	90	58
7	984	18	−11	−13	−5	−5

[a] Angles in degrees. Calculated angles measured from the C_3—C_4 axis away from C_2
[b] Values in polyethylene, from Ref. [2]

BLYP/6-311G(3d,p) calculation for the nonplanar geometry (990 and 1000 cm^{-1}), but not for the planar geometry (both nearly the same, 1000 cm^{-1}). Perhaps this is a coincidence, since the differences are small, but we shall show later that there are two other vibrations for which the agreement with the best calculated frequencies is better if the geometry is taken to be nonplanar.

3. The assignments of the 1612 cm^{-1} vibration as the a_1 symmetric combination of the C═C stretches (along with the C—C stretch) and the 1633 cm^{-1} vibration as their the b_2 antisymmetric combination, based on IR polarization measurements, agree nicely with the now observed Raman intensities, where the former, observed at 1613 cm^{-1}, is the strongest peak in the spectrum and the latter is too weak to be observed (the value 1602 cm^{-1} listed in [3] for the IR peak may be a misprint as we have now verified by repeating the measurement; the other authors [7, 15] reported 1612 cm^{-1}).

It is noteworthy that the scaled HF and post-HF ab initio methods calculate the a_1 and b_2 frequencies too close together and do not permit a statement as to which one is at higher frequency. In contrast, the DFT procedure reproduces their separation well (if anything, exaggerates it) and orders them correctly. We believe that this provides further support for our a priori predicted carbon backbone stretching force constants.

The Ar matrix IR spectrum of the major conformer agreed well with that reported previously [1–3], and so did the spectrum of the minor conformer, with the single exception of the very weak peak at 530 cm^{-1}. While in Refs. [1–3] we reported that there is a weak peak of the minor conformer at 530 cm^{-1} on the side of the much stronger main peak of the major conformer in this region, located at 537 cm^{-1}, the better resolved present spectrum (Fig. 5) convinced us that all peaks in the 520–540 cm^{-1} region are due to the major conformer. The error was caused by insufficient resolution combined with the proximity of the two peaks of very different intensity. As shown in Fig. 5, after irradiation of a matrix containing an isomer mixture with light from a KrF excimer laser the peaks of the major conformer increased while those of the minor conformer decreased and disappeared completely after 1 h. In the difference spectrum (trace c) this is documented by the negative peaks at 730, 914, and 995 cm^{-1}. In contrast, the small peaks at 530 cm^{-1} increase along with others attributed to the major isomer, such as the relatively strong 537 cm^{-1} peak, and like the latter, they therefore appear positive in the difference spectrum. The ratio of their intensity to that of the 537 cm^{-1} peak remains constant throughout. These are clearly peaks of the major conformer and are probably matrix site satellites of the 537 cm^{-1} peak. The results of the scaled ab initio method and DFT also support this analysis.

Finally, we return to the issue of the gauche or cis geometry of the minor conformer. This cannot be resolved by reference to the intensity of vibrations that are of a_2 symmetry at the planar geometry and thus forbidden in an isolated molecule, since matrix perturbations will make them weakly allowed (all three, 730, 920 and 996 cm^{-1} appear in the IR spectrum weakly and polarized perpendicular to the C—C bond [3]). It is, however, reasonable to ask whether the calculated frequencies agree better for one or the other geometry. We have calculated the rms of frequencies for each ab initio method compared with experiment. Since the ab initio calculated frequency of the ν_{13} mode of the s-cis conformer is imaginary, it was not included in the rms calculations. Not surprisingly, the two sets of frequencies at the gauche and s-cis geometries are similar overall. Because of their large rms, unscaled post-HF frequencies cannot be used to distinguish between the two geometries. The scaled HF frequencies by Wiberg and Rosenberg [8] show rms values of 24 cm^{-1} and 27 cm^{-1} for the gauche and s-cis geometries, respectively. Since the difference between the two rms values is only 3 cm^{-1}, it is impossible to derive any conclusion merely based on this result. The corresponding rms values by DFT are 7.4 cm^{-1} and 17.5 cm^{-1}, respectively, (without C—H stretching). Therefore, the results of DFT agree better with the gauche geometry. We have also calculated the rms as a function of torsional angle (τ) along the C—C single bond (Fig. 6). The minimum position is very close to the energy minimum calculated at the gauche form.

The change in the rms error is primarily due to only three modes, and most of the frequencies of the minor rotamer are insensitive to the dihedral angle along the C—C single bond. These are the 983 cm^{-1}, 596 cm^{-1} and 470 cm^{-1} vibrations. The dispersions of these bands as a function of torsional angle calculated with BLYP/ 6-311G(3d,p) theory are presented in Figs. 7 and 8. The peak at 983 cm^{-1} (Fig. 8a) is composed of C═C double bond torsions (~90%) and C—C single bond torsion (~3%) modes. Since π conjugation is a function of torsional angle (τ), the dependence of this frequency on τ is easy to understand. The peak at 596 cm^{-1} is assigned to CH_2 rocking (48%) and CCC deformation (20%). The peak at 470 cm^{-1} is assigned to CH_2 wagging (42%) and

Table 6. Theoretical and experimental frequencies of *s-cis* and *gauche* 1,3-butadiene (in cm^{-1})[a]

	Symmetry		BLYP/ 6-311G(3d,p)	MP2/ 6-31G*[b]	MP2/ DZP[c]	CISD/ DZd[d]	HF/6-13G (scaled)[e]	Exp.[f]	Exp.[g]
gauche	*a*	ν_1	3137	3312	3329	3352	3110		3035
		ν_2	3059	3210	3236	3270	3035		3023
		ν_3	3046	3223	3216	3248	3024		2990
		ν_4	1602	1712	1694	1773	1641	1613	1612[h]
		ν_5	1428	1510	1493	1529	1464	1428	1425
		ν_6	1313	1369	1341	1381	1313		
		ν_7	1041	1098	1072	1102	1057	1034	
		ν_8	990	1019	1007	1042	1004	983	984
		ν_9	901	930	889	964	943		920
		ν_{10}	858	915	905	918	859		
		ν_{11}	733	762	748	777	733	732	730
		ν_{12}	269	278	273	285	281		
		ν_{13}	151	185	184	175	151	136[i]	
	b	ν_{14}	3135	3310	3328	3350	3108		3103
		ν_{15}	3055	3218	3211	3243	3028		3070
		ν_{16}	3033	3202	3325	3256	3014		3010
		ν_{17}	1635	1715	1688	1762	1645		1633
		ν_{18}	1406	1476	1453	1493	1431	1401	1403
		ν_{19}	1280	1336	1310	1350	1284		
		ν_{20}	1081	1125	1101	1135	1101	1089	1087
		ν_{21}	1000	1006	1031	1062	1017		996
		ν_{22}	902	931	882	958	946		914
		ν_{23}	600	631	622	644	619	584	596
		ν_{24}	464	471	463	474	455	470	470
Rms			26.2 (7.4)	129.8 (53.8)	143.9 (42.3)	160.2 (81.8)	23.5 (24.1)		
s-cis	a_1	ν_1	3139	3312	3330	3353	3113		3035
		ν_2	3064	3228	3243	3277	3043		3023
		ν_3	3056	3217	3321	3254	3029		2990
		ν_4	1596	1706	1689	1767	1637	1613	1612[h]
		ν_5	1429	1515	1495	1534	1466	1428	1425
		ν_6	1327	1392	1361	1403	1331		
		ν_7	1039	1091	1064	1093	1045	1034	
		ν_8	855	907	898	910	852		
		ν_9	288	309	296	307	302		
	a_2	ν_{10}	1001	1019	989	1034	1019		996
		ν_{11}	895	907	828	923	935		920
		ν_{12}	725	739	705	756	728	732	730
		ν_{13}	125i	163i	168i	162i	146i		136i
	b_1	ν_{14}	1000	1041	1026	1061	1018	983	984
		ν_{15}	900	922	849	942	941		914
		ν_{16}	500	521	501	525	498	470	470
	b_2	ν_{17}	3137	3309	3327	3349	3109		3103
		ν_{18}	3058	3218	3227	3259	3032		3070
		ν_{19}	3042	3207	3215	3246	3020		3010
		ν_{20}	1639	1721	1694	1769	1653		1633
		ν_{21}	1409	1480	1456	1496	1437	1401	1403
		ν_{22}	1285	1343	1319	1358	1289		
		ν_{23}	1087	1137	1114	1146	1109	1089	1087
		ν_{24}	557	570	560	576	568	584	596
Rms			32.1 (17.5)	132.4 (57.7)	147.7 (52.8)	161.6 (80.8)	27.1 (27.1)		

[a] The numbers in parentheses are rms without CH stretching modes
[b] Taken from Ref. [9, 10]
[c] Taken from Ref. [36]
[d] Taken from Ref. [37]
[e] Taken from Ref. [33]
[f] Argon matrix, Raman, this work
[g] Argon matrix, IR. Taken from Ref. [3]
[h] The value 1602 cm^{-1} listed in Ref. 3 is a misprint (see text)
[i] Gas phase, taken from Ref. 38

CH_2 rocking (28%). The corresponding dispersion curves are presented in Fig. 8b. It can be seen that the dispersion is as large as 40 cm^{-1} between the two conformations. The agreement is clearly worse for the s-cis planar geometry than for the nonplanar gauche geometry. It would be quite a coincidence for the three vibrations to be calculated incorrectly by just the right amount to change this result, or for matrix shifts to change it. Yet, the polarization data leave no doubt that the IR transition moments in the minor conformer (but

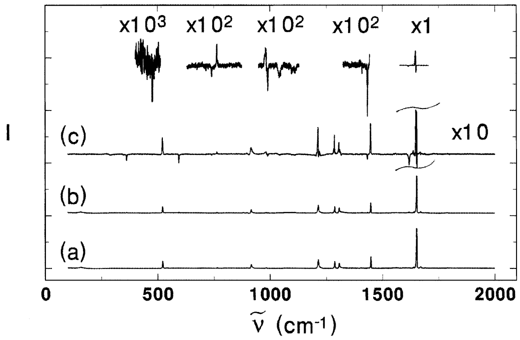

Fig. 2. Raman spectra of 1,3-butadiene conformers in an Ar matrix at 18 K. Trace *a* after deposition from room-temperature gas; trace *b* after deposition from hot gas; trace *c* the difference *a–b*, enlarged tenfold

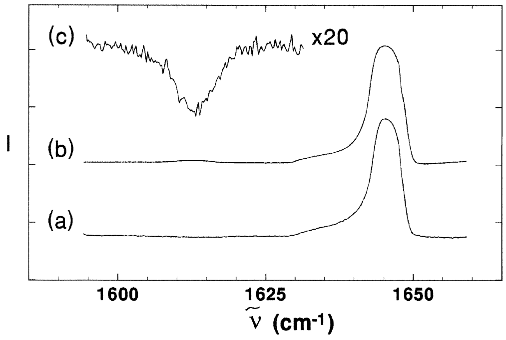

Fig. 3. Raman spectra of 1,3-butadiene conformers in an Ar matrix at 18 K. Trace *a* after and trace *b* before 248-nm irradiation of conformer mixture deposited from hot gas; trace *c* the difference *a–b*, enlarged 20-fold. Spectral slit width: 6 cm^{-1}

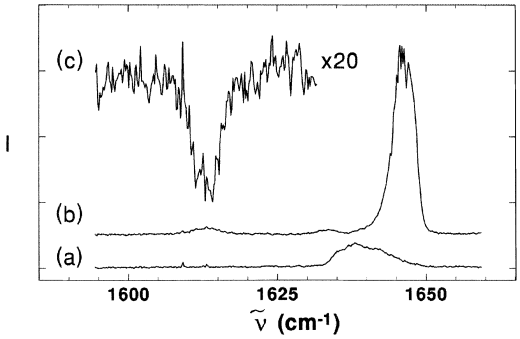

Fig. 4. Raman spectra of 1,3-butadiene conformers in an Ar matrix at 18 K. Trace *a* after and trace *b* before annealing of conformer mixture deposited from hot gas; trace *c* the difference *a–b*, enlarged 20-fold. Spectral slit width: 4 cm^{-1}

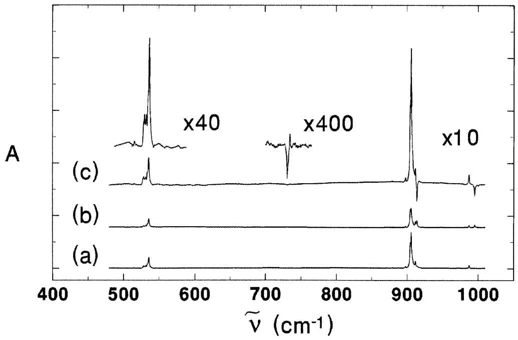

Fig. 5. FT-IR spectra of 1,3-butadiene conformers in an Ar matrix at 18 K. Trace *a* after and trace *b* before 248-nm irradiation of conformer mixture deposited from hot gas; trace *c* the difference

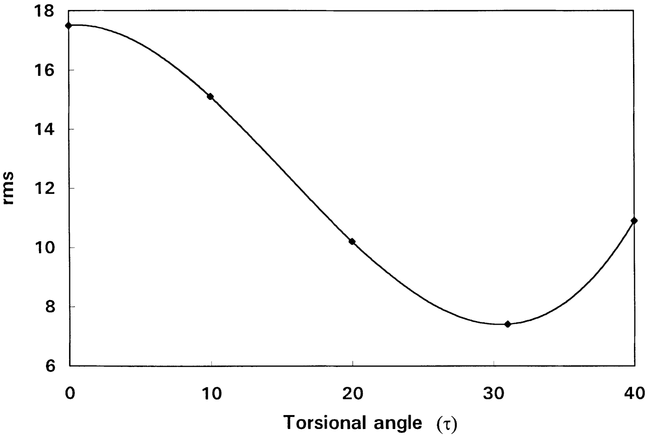

Fig. 6. The root mean square (*rms*) error in reciprocal centimeters as compared with experiment as a function of torsional angle (τ)

not the C_{2h} major conformer, where they were obtained by the same procedure) are all mutually parallel or perpendicular. This could happen only by an even much larger coincidence if the molecule were not planar. So far, all calculations predict that the angles of several transition moments will deviate strongly from 0 or 90° at the optimized nonplanar geometry.

Several methods of calculation [3] including the present CCD/6-311G(d,p) method, yield accurate transition dipole moments for the trans conformer, and appear trustworthy. Similar calculations were done with the CCD/6-311G(d,p) method for the s-gauche conformer at a twist angle of 30°. The calculated transition moment directions of the observed peaks at 984, 1089, 1401 and 1612 cm^{-1} are 46, 15, 61 and 42°, respectively. These values deviate significantly from the observed values of 0 or 90°, confirming the earlier conclusion that the actual conformation of the minor conformer in the matrix should be planar or near-planar.

4 Conclusions

We have attempted a priori predictions of harmonic vibrational properties of 1,3-butadiene with DFT using several density functionals in combination with various basis sets. The harmonic vibrational frequencies are successfully reproduced with BLYP/6-311G(3d,p). Without C—H stretching modes, the rms compared with experiment is 8.9 cm^{-1}. Based on these results, we have suggested new C—C, C=C, C—C/C=C and C=C/C=C stretching force constants of *s-trans*-1,3-butadiene as 5.01, 8.68, 0.52 and −0.16 mdyne/Å, respectively. Our suggested C—C and C=C stretching force constants are

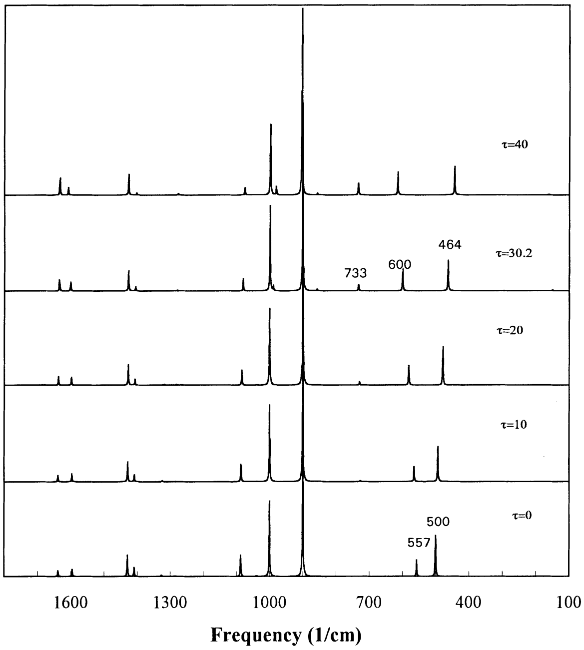

Fig. 7. Predicted IR spectra of the cis and gauche butadienes as a function of torsional angle (τ)

close to the scaled ab initio results [17, 19, 33, 34]. The C—C/C=C and C=C/C=C coupling constants are larger then those for HF and MP calculations, but close to scaled HF/MIDI-4 results of Kofranek et al. [19]

The APT components of *s-trans*-1,3-butadiene calculated by DFT are in good agreement with observed IR intensities but not with transition moment directions. There are sign disagreements in the *xy* component of the C$_1$ atom and in the *xx* component of the H$_7$ atom APT, although these values are relatively small in magnitude. Inclusion of diffuse functions in the basis set increases the *zz* component (out-of plane motion) of the APT resulting in overestimation of the infrared intensities of the a_u modes. The predicted vibrational frequencies and infrared intensities are insensitive to the kind of polarization functions used with the triple-zeta basis set.

The rms errors of predicted vibrational frequencies of *gauche*- and *s-cis*-1,3-butadienes are calculated as 26.2 cm^{-1} and 32.1 cm^{-1}, respectively, compared with experiment. Without C—H stretching frequencies, the rms values are reduced to 7.4 cm^{-1} and 17.5 cm^{-1}, respectively. This observation is related to the strong dispersions of the peaks at 983 cm^{-1}, 596 cm^{-1} and 470 cm^{-1} with respect to the torsional angle calculated by DFT, all of which yield better agreement for the gauche geometry. Yet, even at the CCD/6-311G(d,p) level, the transition dipole moment directions are only compatible with C_{2v} symmetry for the minor conformer.

Two conclusions are possible: either

1. The better agreement of the calculated frequencies for the nonplanar form is coincidental and the matrix isolated molecule is planar, or
2. The molecule is indeed nonplanar but tunnels rapidly between the two mirror-image forms on the IR time scale, (or the barrier is so low that the lowest vibrational level already lies above it).

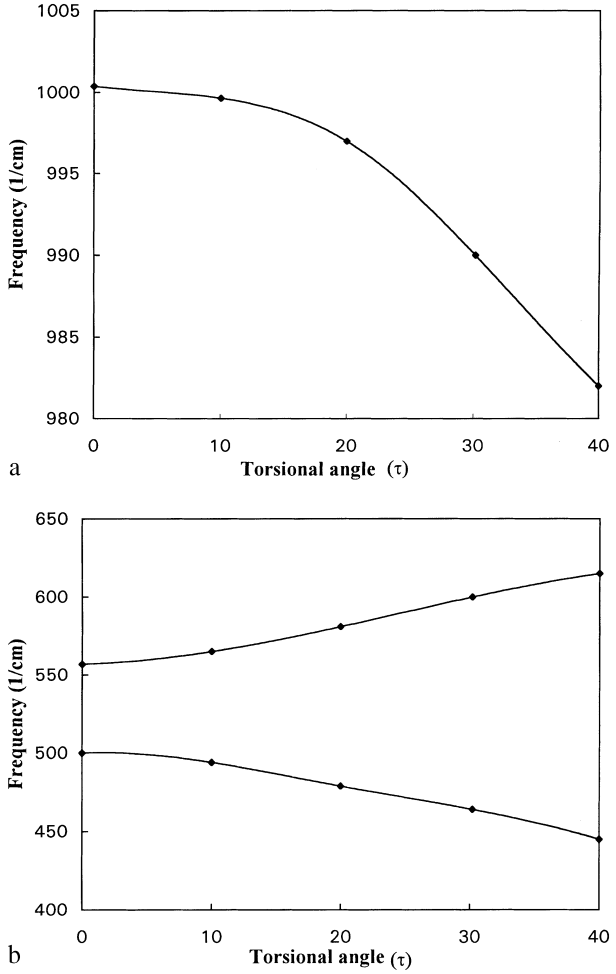

Fig. 8a,b. The calculated frequency dispersion with respect to the torsional angle (τ). **a** The 990 cm^{-1} vibration, **b** the 464 cm^{-1} and 600 cm^{-1} vibrations

Possibility 2 has been considered [3] and judged unlikely but now appears a little more attractive than before. If correct, it would be quite interesting and would suggest some intriguing gas-phase experiments.

Acknowledgements. We thank the National Science Foundation (CHE-9601976) for support to the Georgetown Molecular Modeling Center, and the National Center for Supercomputing Applications (NCSA, no. CHE-970017N) for the use of supercomputing facilities. Work at Boulder was supported by a grant from the National Science Foundation, CHE-9318469. We are grateful to Dr. T. F. Magnera for assistance.

References

1. Fisher JJ, Michl J (1987) J Am Chem Soc 109:1056
2. Arnold BR, Balaji V, Downing JW, Radziszewski JG, Fisher JJ, Michl J (1991) J Am Chem Soc 113:2910
3. Arnold BR, Balaji V, Michl J (1990) J Am Chem Soc 112:1808
4. Squillacote ME, Sheridan RS, Chapman OL, Anet FAL (1979) J Am Chem Soc 101:3657

5. Aston JG, Szasz G, Woolley HW, Brickwedde FG (1946) J Chem Phys 14:67
6. Lipnick RL, Garbisch EW Jr (1973) J Am Chem Soc 95:6370
7. Furukawa Y, Takeuchi H, Harada I, Tasumi M (1983) Bull Chem Soc Jpn 56:392
8. Wiberg KB, Rosenberg RE (1990) J Am Chem Soc 112:1509
9. Guo H, Karplus M (1991) J Chem Phys 94:3679
10. Murcko MA, Castejon H, Wiberg KB (1996) J Phys Chem 112:16162
11. Feller D, Davidson ER (1985) Theor Chim Acta 68:57
12. Kofranek M, Karpfen A, Lischka H (1992) Chem Phys Lett 189:281
13. Cole ARH, Green AA, Osborne GA (1973) J Mol Struct 48:212
14. Panchenko YN (1975) Spectrochim Acta Part A 31:1201
15. Huber-Walchli P, Gunthard HH (1981) Spectrochim Acta Part A 37:285
16. Fogarasi G, Pulay P (1985) In: Durig JR (ed) Vibrational spectra and structure. Elsevier, New York
17. Szalay PG, Karpfen A, Lischka H (1987) J Chem Phys 87:3530
18. Kofranek M, Karpen A, Lischka H (1990) Int J Quantum Chem 24:721
19. Kofranek M, Lischka H, Karpfen A (1992) J Chem Phys 96:982
20. Tang W, Bally T (1993) J Phys Chem 97:4365
21. Vijay A, Sathyanarayana DN (1994) J Mol Struct 311:87
22. Lee JY, Hahn O, Lee SJ, Choi HS, Shim H, Mhin BJ, Kim KS (1995) J Phys Chem 99:1913
23. Kohn W, Sham LJ (1965) Phys Rev A 140:1133
24. (a) Bérces A, Ziegler T (1993) J Chem Phys 98:4793; (b) Brooks CL III, Case DA (1993) Chem Rev 93:2487; (c) Johnson BG, Gill PMW, Pople JA (1993) J Chem Phys 98:5612; (d) Oie T, Topol IA, Burt SK (1994) J Phys Chem 98:1121; (e) Pulay P (1995) J Mol Struct 347:293
25. Frisch MJ, Trucks GW, Schlegel HB, Gill PMW, Johnson BG, Robb MA, Cheeseman JR, Keith TA, Petersson GA, Montgomery JA, Raghavachari K, Al-Laham MA, Zakrzewski VG, Ortiz JV, Foresman JB, Cioslowski J, Stefanov BB, Nanayakkara A, Challacombe M, Peng CY, Ayala PY, Chen W, Wong MW, Andres JL, Replogle ES, Gomperts R, Martin RL, Fox DJ, Binkley JS, Defrees DJ, Baker J, Stewart JJP, Head-Gordon M, Gonzalez C, Pople JA (1995) Gaussian 94, revision C.2, Gaussian, Pittsburgh Pa
26. (a) Rauhut G, Pulay P (1995) J Phys Chem 99:3093; (b) Baker J, Jarzecki AA, Pulay P (1998) J Phys Chem 102:1412
27. Vosko SH, Wilk L, Nusair M (1980) Can J Phys 58:1200
28. Lee C, Yang W, Parr RG (1988) Phys Rev B 37:785
29. Becke AD (1988) Phys Rev A 38:3098
30. Becke AD (1993) J Chem Phys 98:1372
31. Person WB, Zerbi G (eds.) (1982) Vibrational intensities in infrared and Raman spectroscopy. Elsevier, Amsterdam
32. Hemley RJ, Brooks BR, Karplus M (1986) J Chem Phys 85:6550
33. Bock CW, Panchenko YN, Krasnoshchiokov SV, Pupychev VI (1985) J Mol Struct 129:57
34. Bock CW, Panchenko YN, Pupyshev VI (1990) J Comput Chem 11:623
35. Bock CW, Trachtman M, George P (1980) J Mol Struct 84:243
36. Rice JE, Liu B, Lee TJ, Rohlfing CM (1989) Chem Phys Lett 161:277
37. Alberts IL, Schaefer HF III (1989) Chem Phys Lett 161:375
38. Carreira LA (1975) J Chem Phys 62:3851